J. Chem. Sci. (2020) 132:10
https://doi.org/10.1007/s12039-019-1699-1

REGULAR ARTICLE

Effect of aggregated Aβ protofilaments on intermolecular vibrational spectrum of confined water

PRABIR KHATUA[a], SOUVIK MONDAL[a] and SANJOY BANDYOPADHYAY[a,b,*]
[a]Molecular Modeling Laboratory, Department of Chemistry, Indian Institute of Technology, Kharagpur, Kharagpur 721302, West Bengal, India
[b]Centre for Computational and Data Sciences, Indian Institute of Technology, Kharagpur, Kharagpur 721302, West Bengal, India
E-mail: sanjoy@chem.iitkgp.ac.in

MS received 11 July 2019; revised 26 August 2019; accepted 27 August 2019

Abstract. Alzheimer's disease, one of most common neurodegenerative diseases, is believed to be caused due to the self-assembly of amyloid beta (Aβ) peptides into insoluble fibrils in the brain. Atomistic molecular dynamics simulations have been carried out to probe the effects of non-uniform structural distortions of aggregated Aβ_{17-42} protofilaments of different sizes, ranging from pentamer to tetradecamer, on the low-frequency vibrational spectrum of water confined within their amphiphilic nanocores. The calculations revealed increased back scattering of water molecules present either at the exterior surfaces of the protofilaments or confined within their cores, thereby leading to blue shifts of the band corresponding to O $\cdots$ O $\cdots$ O bending or restricted transverse motions of water. Due to more restricted environment, the effect is more for the core water molecules. It is observed that the extent of such shifts is sensitive to the degree of confinement within the protofilament cores and the nature of hydrogen bonding. Importantly, the structural crossover of the protofilaments with increased core volume at decamer has been found to be associated with characteristic effect on the low-frequency modes of the water molecules confined within its core.

Keywords. Alzheimer's disease; molecular dynamics simulations; amyloid beta (Aβ); vibrational spectrum and core water.

1. Introduction

Protein folding abnormalities are associated with several life-threatening diseases including Alzheimer's disease, Parkinson's disease, type II diabetes, etc.[1,2] The primary cause of such diseases is the formation of soluble oligomers or insoluble fibrils, termed as "amyloids",[3] due to self-assembly of proteins. Alzheimer's disease (AD) is by far one of the major threats to the public health affecting million of people worldwide. Accumulation of fibrils primarily composed of amyloid beta (Aβ) peptides in the brain is linked with AD. Aβ peptide is processed from enzymatic cleavage of amyloid precursor protein (APP) by β- and γ-secretases.[4,5] It can be of various lengths depending on the cleavage position of APP. However, there are mainly two predominant components of Aβ peptide containing 40 (Aβ_{40}) and 42 residues (Aβ_{42}) length which are found in the AD affected brains.[5,6] Neurotoxicity induced by the soluble Aβ oligomers and insoluble fibrils is believed to be pathological cause for AD.[7–9] Importantly, there are several experimental reports which have corroborated soluble oligomers to be more neurotoxic rather than the insoluble fibrils.[8,10–12] Therefore, recent research attention has been shifted toward untangling the structural features of soluble Aβ oligomers rather than probing the insoluble fibrils. One important issue that needs to pay an attention is the role played by water in the formation and stabilization of such Aβ oligomers.

A number of studies pointed out the role of water in guiding the conformational features of Aβ peptides and their fibrillation.[13–15] In an important work, Krone *et al.*,[13] demonstrated how water expulsion and hydrophobic collapse drive the formation of stable Aβ_{16-22} aggregates in pre-fibrillar or protofilamentous form. They observed that first a dewetting or drying transition takes place which drives the

*For correspondence

Published online: 19 December 2019

hydrophobic collapse resulting in the formation of fibrils in some of the trajectories. They also noticed these two phenomena occurring on the same time scale. Further, release of structured water from the Aβ peptide surface to bulk has also been shown to drive such hydrophobic collapse from another pioneering study by Thirumalai *et al.*[14] Recently, molecular dynamics (MD) simulation studies have shown that water molecules around the hydrophobic segments of Aβ peptide monomers irrespective of their conformations are loosely bound, and therefore, are expected to be easily removed from the surface of those segments to facilitate the hydrophobic collapse during aggregation.[16] Hydrated hydrophobic cavities have been reported from MD simulation studies in the case of fibrils formed by the larger fragments of Aβ peptide, such as Aβ_{9-40} and Aβ_{17-42} where the peptide adopts a β-strand-loop-β-strand U-shape structure.[17,18] However, none of the experimentally determined structures of Aβ fibrils contain water within the cavities probably due to the limitations of experimental techniques.[19–23] Water molecules are found to be present mostly in the hydrophobic cavity formed by the loop region in both Aβ_{9-40} and Aβ_{17-42} protofilaments. Presence of such water may play an important role in enhancing the stability of the pre-fibrillar structures, as they are expected to neutralize the charges of the residues forming salt-bridge (Asp-23 and Lys-28) inside the core region.[24–26] Furthermore, the confined water molecules present in the hydrophobic cavities have been observed to be translationally and rotationally very stiff as compared to bulk water from MD simulation studies.[27,28] Recently, we have also characterized the presence of water within the nanocores of the Aβ protofilaments.[29,30] Structural and dynamic quantities of these water molecules have been computed and compared among different Aβ protofilaments of varying sizes. It has been demonstrated that properties of water confined within such nanocores are heterogeneous and depend upon the core volume. Based on the findings, it has been proposed that the protein–water hydrogen bonds involving the core water molecules stabilize the aggregates, while breaking of water–water hydrogen bonds inside the cores initiates the required impetus in steering the further growth of the aggregates. Such breaking and formation of hydrogen bonds inside the core region during the growth process are expected to influence the intermolecular vibrational density of states of the confined water in terahertz (THz) and far-infrared (far-IR) regions.[31–34] Thus, we believe that probing the low-frequency intermolecular vibrational spectra of the core water might be an effective alternative tool in monitoring the aggregation process of Aβ peptides.

Experimentally, one can study low-frequency vibrational spectra using Raman, IR, THz spectroscopy, and inelastic incoherent neutron scattering (IINS) techniques. THz spectroscopy has been extensively used in recent times to investigate water dynamics around proteins.[35–39] In an important study, Havenith and coworkers[35] have shown that THz spectroscopy in combination with molecular dynamics (MD) simulations can be an effective tool in probing water dynamics spanned over several hydration layers around proteins and other macromolecules.

In this work, we study the low-frequency vibrational density of states (VDOS) of the water molecules confined within the amphiphilic nanocores of aggregated Aβ_{17-42} protofilaments. In particular, our objective in this study has been to compare the results among five different Aβ protofilaments namely, pentamer (O_5), octamer (O_8), decamer (O_{10}), dodecamer (O_{12}), and tetradecamer (O_{14}) to find out the size dependence, if any. The outline of the rest of the article is as follows. The details of system setup and simulation protocols are described in brief in Section 2. The results obtained from our study have been delineated in Section 3. Finally, the conclusions reached from the study are presented in Section 4.

2. System setup and simulation methods

Two independent MD simulations in aqueous medium with different velocity distributions at a temperature of 300 K for each of five Aβ_{17-42} protofilaments (henceforth represented as Aβ), namely pentamer (O_5), octamer (O_8), decamer (O_{10}), dodecamer (O_{12}), and tetradecamer (O_{14}) have been carried out using the NAMD code.[40] The initial coordinates were taken from NMR spectroscopic data (model 10 of PDB entry 2BEG)[23] for the Aβ pentamer. The higher order protofilaments (O_8 onward) were obtained from the pentameric structure by adding required number of monomer units with an intermonomeric distance of 4.8 Å, where the central chain in model 10 of 2BEG was used as the base unit of the hairpin. Further details of the method adopted are available in our earlier work.[41] Terminal residues, L(17) and A(42), of each of the monomers present in the respective protofilament are considered in standard zwitterionic forms. The individual protofilaments were immersed in orthorhombic cells of appropriate dimensions containing equilibrated water molecules. Required number of counterions was then added by replacing water

molecules to neutralize each of the system. The exact system dimensions and the number of water molecules and ions can be found elsewhere.[41]

After initial energy minimization, the temperature of each of the systems was gradually increased to 300 K within a short MD run of 100 picoseconds (ps) under isothermal-isobaric ensemble (NPT) conditions at a constant pressure of 1 atm. All the systems were then equilibrated under NPT ensemble conditions at a constant pressure of 1 atm and temperature 300 K with positional constraints on the aggregate for 5 nanoseconds (ns) duration followed by release of constraints for another 5 ns. Unconstrained NPT simulation was extended up to $\sim$50 ns for higher order protofilaments (O_8 onward) so as to obtain more stable equilibrated configurations. Afterward, the equilibration simulation conditions were changed from constant pressure and temperature (NPT) to that of constant volume and temperature (NVT) for 5 ns followed by a long NVT production run of 110 ns duration. The temperatures of the systems were controlled by using the Langevin dynamics method with friction constant 1 ps^{-1}, while the Nosé-Hoover Langevin piston method was utilized for controlling the pressure.[42]

All the simulations were performed with an integration time step of 1 femtosecond (fs), and the trajectories were stored with a frequency of 400 fs. Constraints were applied on the bonds involving the hydrogen atoms by using the SHAKE algorithm.[43] We have employed the minimum image convention[44] to compute the short-range Lennard-Jones interactions with a spherical cutoff distance of 12 Å and a switch distance of 10 Å, while long-range electrostatic interactions were calculated using the particle-mesh Ewald method.[45] In the calculations, we have used all-atom CHARMM22 force field with CMAP corrections for the peptide,[46,47] while mTIP3P[48] model (modified version of TIP3P[49]) which is consistent with the chosen peptide force field was used for water. Note that, portions of the trajectories were re-run and stored with a higher resolution of 1 fs for computing low-frequency vibrational spectra.

3. Results and Discussion

In a recent work,[30] we studied in detail the effect of nonuniform structural distortions of Aβ protofilaments with varying size (pentamer to tetradecamer) on the diffusivity and hydrogen bonding environment of the water molecules confined within their amphiphilic nanocores. It was demonstrated that the non-uniform confinement within the cores of the protofilaments results in heterogeneously restricted water dynamics within those. The degree of restriction was found to depend on the available core volume. Importantly, structural crossover of the aggregates for the decamer as demonstrated in our earlier reports[29,41] was found to be associated with dynamical transition of water confined within its core. Besides, a direct one-to-one correlation between the heterogeneously restricted core water mobilities and the kinetics of breaking and formation of hydrogen bonds was observed which clearly corroborated that the modified hydrogen bond arrangement within the cores of higher order Aβ protofilaments is the origin behind the crossover in core water mobility. Such heterogeneous water dynamics associated with dynamical crossover for the core water of the decamer is also expected to influence low-frequency vibrational density of states (VDOS) of the confined water. In this work, we attempt to probe the effect of size of the Aβ aggregates on the low-frequency vibrational spectrum of the core water molecules. A simple geometric approach has been used to identify the "core" water. According to this approach, we first consider two surfaces formed by the two arms (first arm: Phe-20 to Asn-27 and second arm: Ala-30 to Met-35) of the peptide β-hairpin units of the protofilament. Then, all possible vectors $\overrightarrow{AB}$ formed between the C_α atoms of these two surfaces that would eventually be used to define core water are constructed. A tagged water molecule is said to be a core water if it fulfills the following two criteria. According to the first criterion, the perpendicular distance of the tagged water oxygen atom ($\overrightarrow{O}$) to any one of the $\overrightarrow{AB}$ vectors is within 0.5 Å, while the second criterion is that both $\angle OAB$ and $\angle OBA$ for that particular vector $\overrightarrow{AB}$ have to be within 90°. It may be noted that we have restricted the area confined within Phe-20 to Met-35 in defining core water. Besides, the two terminal peptide monomers of the protofilaments are not considered in the calculation to avoid possible artifacts in the results due to their greater flexibility as compared to the non-terminal peptides. The results obtained are compared with that for the surface water molecules. As mentioned earlier,[29,30] water molecules those are found within 5 Å from the aggregates (excluding the core region) are defined as the "surface" water. VDOS of the water molecules is calculated by Fourier transformation of the corresponding velocity autocorrelation function (VACF). VACF is defined as

$$C_V(t) = \frac{\langle \vec{v}_i(t).\vec{v}_i(0)\rangle}{\langle \vec{v}_i(0).\vec{v}_i(0)\rangle} \quad (1)$$

where, $\vec{v}_i(t)$ is the velocity vector of the atom of type i (O or H for a water molecule) at time t. The angular brackets denote that the results are averaged over all the atoms of a particular type and over different reference initial times.

We have calculated the VACF for the oxygen ($C_V^O(t)$) and the hydrogen ($C_V^H(t)$) atoms of the water molecules confined in and around the Aβ aggregates with different sizes. The results for the core water molecules of the five Aβ protofilaments are shown in Figure 1. The corresponding data for the surface water as obtained by averaging over all the protofilaments are incorporated in the figure for comparative analysis. It may be noted that consistent with earlier reports on water properties,[29,30] the identical environment at the exterior surfaces of the protofilaments also results in near-homogeneous VACF of surface water. Therefore, as done before,[29,30] we present the data for the surface water molecules as obtained by taking an average over all the protofilaments. The corresponding functions for pure bulk water calculated from an additional MD simulation of mTIP3P water following similar conditions as that described in Section 2 are also included in the figure as a reference. In general, the relaxation of the function $C_V^O(t)$ is characterized by a negative dip separated by a bump. This is known as the 'caging' effect, which arises due to back-scattering of the water oxygen atoms on collisions with their neighbors. Besides, it can be seen that the function $C_V^O(t)$ for the water molecules confined within the cores or at the exterior surfaces of the protofilaments exhibit deeper minima as compared to that for pure bulk water. This is consistent with the relatively rigid water layers in and around the protofilaments, as reported in our recent work.[30] It is apparent from the figure that the extent of the caging effect is significantly higher for the core water due to constrained environment within the protofilament core. Importantly, the data reveal that such caging effect for the core water is heterogeneous among the Aβ aggregates due to non-uniform confinement. In accordance with earlier reports,[29,30] maximum caging effect is noticed for the lower order protofilaments (O_5 and O_8) due to their relatively compact structures. On the other hand, the extent of caging effect decreases with the increase of the aggregate size for the higher order protofilaments (O_{10} onward). Interestingly, the effect is found to be minimum for the core water present in O_{10}. We showed recently that beyond a critical size (O_{10} in this case), the protofilaments undergo structural distortions due to twisting of the Aβ monomers to search for more stable structures.[41] Such structural distortion of the higher order protofilaments leads to reduction in confinement due to increased available core dimension,[29] maximum reduction being observed for the crossover protofilament, O_{10}. Thus, the anomalous caging effect for O_{10} core water as observed in the present study is an important finding which is consistent with earlier reports.[29,30] The VACF for water hydrogen atoms ($C_V^H(t)$) reveals a general oscillatory nature of the function with relatively more deeper minima in each case as compared to $C_V^O(t)$. Note that $C_V^H(t)$ provides information about the librational motions (hindered rotations) of water. The present result indicates a stronger caging effect on water librations. It can be further noticed that water

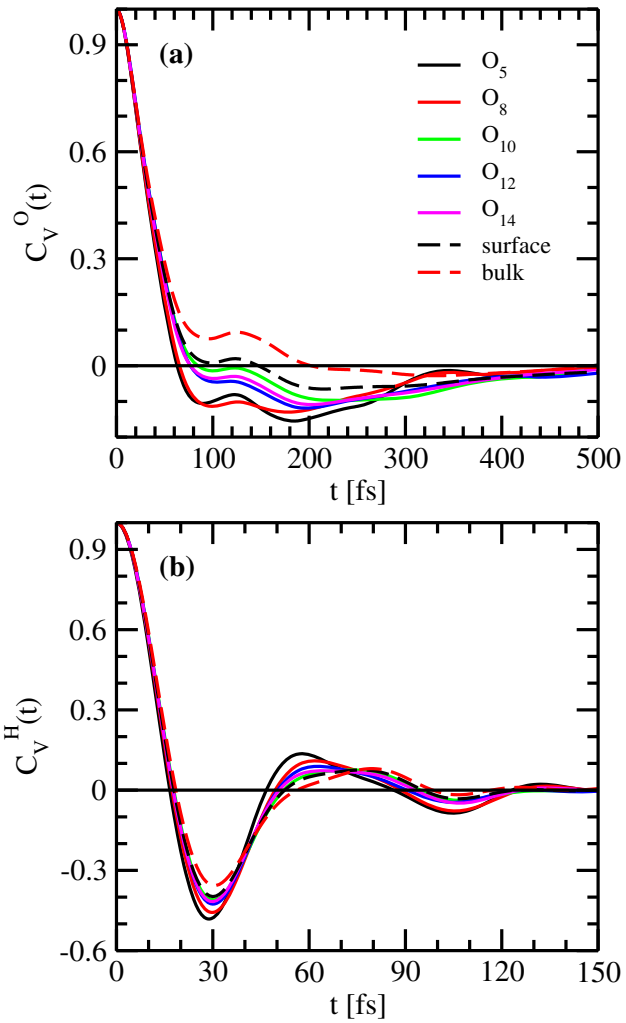

Figure 1. (a) Velocity autocorrelation function, $C_V^O(t)$, for the oxygen atoms of the water molecules that are present within the cores of different Aβ protofilaments. (b) The corresponding function, $C_V^H(t)$, for the hydrogen atoms of those water molecules. The respective results for the surface water molecules as obtained by averaging over the protofilaments and that for water in pure bulk state are shown in each of the panels for comparison.

molecules present at the exterior surface of the Aβ protofilaments exhibit relatively deeper minima as compared to water in pure bulk state. Expectedly, such minima are found to be even more deeper for the core water. However, we do not find any noticeable difference between water confined within the core and that present at the exterior surface of O_{10}. It suggests that the core topology of O_{10} provides a critical environment where the behavior of water is nearly similar to that of its surface water, thereby allowing easy exchange of water between the core and surface. Such possibility of easy exchange of water has been demonstrated in our earlier work,[30] where it was proposed that diffusion of a fraction of water molecules forming short-lived water–water hydrogen bonds within the crossover protofilament decamer initiates the required impetus in steering further growth of the Aβ protofilament.

Recently, we demonstrated that water molecules irrespective of whether they are confined within the cores or present at the exterior surfaces of the Aβ protofilaments exhibit strong propensity to form protein–water (PW) hydrogen bonds with longer relaxation times.[30] Such propensity was found to be markedly stronger for the core water. Furthermore, it was also shown that the core water molecules form stronger water–water (WW) hydrogen bonds in comparison to that in pure bulk state. Importantly, slow long-time relaxations of PW and WW hydrogen bonds formed by the core water molecules were found to be the origin behind their hindered translational and rotational motions. Therefore, it would be compelling to explore the influence of formation of hydrogen bonds on the VACFs of those bound water molecules, if any. This is done by re-calculating the functions $C_V^O(t)$ and $C_V^H(t)$ for only those water molecules that are bound to the Aβ peptides of the protofilaments by PW hydrogen bonds. We have employed geometric conditions[30,50,51] to define PW and WW hydrogen bonds. According to the first condition, to form a PW hydrogen bond the distance between a tagged donor or acceptor Aβ peptide atom and the oxygen atom of a water molecule should be within 3.3 Å. The second condition for a peptide acceptor atom (X) to form a PW hydrogen bond is that the angle between one of the O–H bond vectors of the water and the vector joining the water oxygen atom and X be within 35°. Similarly, for a donor atom of the peptide (Y) to form a PW hydrogen bond, the angle between the Y–H bond vector and that connecting Y and the water oxygen should be within 35°. On the other hand, two water molecules are said to form a WW hydrogen bond if the inter-oxygen and non-bonded oxygen–hydrogen distances are found to be within 3.5 Å and 2.45 Å, respectively, and the oxygen–oxygen–hydrogen angle is less than 30°.[30] The results for the water molecules present within the amphiphilic nanocores of the five different protofilaments are shown in Figure 2. The corresponding results for the surface water molecules as obtained by averaging over all the protofilaments along with that for water in pure bulk state are marked in the figure. A distinct difference between the $C_V^O(t)$ functions for the water molecules that are bound to the protofilaments by PW hydrogen bonds and that of all confined water molecules as discussed before

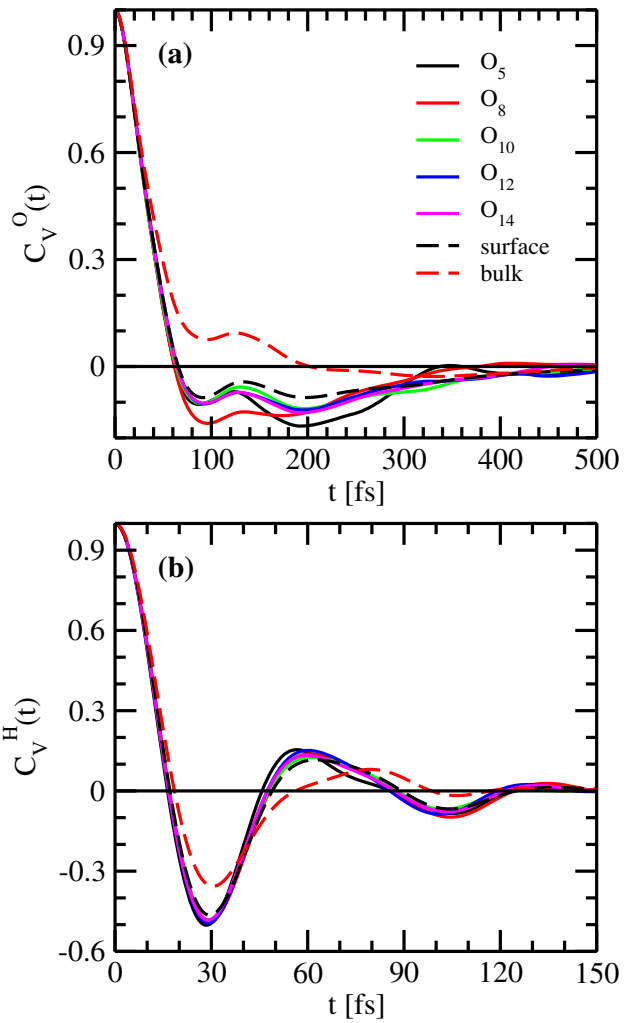

Figure 2. (a) Velocity autocorrelation function, $C_V^O(t)$, for the oxygen atoms of the water molecules that are hydrogen bonded with the peptide atoms and present within the cores of different Aβ protofilaments. (b) The corresponding function, $C_V^H(t)$, for the hydrogen atoms of such bound water molecules. The respective results for the surface water molecules as obtained by averaging over the protofilaments and that for water in pure bulk state are shown in each of the panels for comparison.

(see Figure 1(a)) is visible. As before, all the decay curves exhibit deeper minima compared to that of bulk. However, the depth of the minima is significantly higher as compared to that observed in Figure 1(a), where all the water molecules were considered. These observations are true irrespective of whether the water molecules are confined within the core regions or are at the exterior surfaces of the protofilaments. It is a signature of increased rigid environment with enhanced caging effects for the bound water molecules, and is a direct consequence of stronger PW hydrogen bonds and their sluggish dynamics as reported in our previous work.[30] In fact, it can be seen that the depth of the minima in the $C_V^O(t)$ plots as observed here correlates well with the time scale of hydrogen bond dynamics.[30] Interestingly, no noticeable difference in the function $C_V^O(t)$ for the core water in O_5 between Figures 1(a) and 2(a) is observed. This is due to the fact that most of the water molecules confined within O_5 core form PW hydrogen bonds. On the other hand, due to the formation of hydrogen bonds with the protofilaments, water librational motions in and around the protofilaments become almost identical among themselves as evident from the decay curves of $C_V^H(t)$ in Figure 2(b). Homogeneous relaxation patterns of the decay curves as observed for core and surface water molecules illustrate that librational motions of the water present within the cores are either unaffected or marginally affected due to the formation of PW hydrogen bonds with the protofilaments.

It is experimentally known that the low-frequency intermolecular vibrational spectrum of water is characterized by two broad bands around $\sim 50\,\mathrm{cm}^{-1}$ and $\sim 200\,\mathrm{cm}^{-1}$, respectively, under ambient conditions.[31,32,34,52,53] In general, the band around $50\,\mathrm{cm}^{-1}$ corresponds to the O···O···O bending mode originating from triplets of hydrogen bonded water molecules, whereas the $200\,\mathrm{cm}^{-1}$ band is attributed to O···O stretching mode arising from longitudinal oscillations of hydrogen bonded pairs of water molecule.[31,32] Ambiguity often arises over the interpretation of the origin of the $50\,\mathrm{cm}^{-1}$ band, since the vibrational spectra of several non-hydrogen-bonded liquids also contain this band.[33,54] Therefore, it is suggested that this band is not necessarily associated with hydrogen bonds. Rather, it arises due to restricted transverse oscillations along all directions within the local caged environment of the tagged water molecules.[54] Importantly, our calculation reveals existence of water triplets forming O···O···O bending, both within the core and at the exterior surface of the aggregated protofilaments. A representative snapshot of the pentamer (O_5) highlighting its core and exterior water molecules that are involved in O···O···O bending is shown in Figure 3. It may be noted that besides these two intermolecular bands in the low-frequency VDOS of water, there exists a third band at $\sim 500\,\mathrm{cm}^{-1}$, which corresponds to water librational motions as demonstrated from infrared (IR) spectroscopy,[34] and simulation studies.[55]

We have calculated the power spectra $S_O(\omega)$ and $S_H(\omega)$ for the water molecules present in and around the Aβ protofilaments. This is done by taking Fourier cosine transform of the corresponding VACF ($C_V^O(t)$ and $C_V^H(t)$). The results for water molecules confined within the cores of the Aβ protofilaments are presented in Figure 4. The corresponding average data for the water present at the exterior surfaces of the protofilaments and that for water in pure bulk state are also incorporated in the figure for comparative analysis. It can be seen from Figure 4(a) that the $\sim 50\,\mathrm{cm}^{-1}$ band corresponding to O···O···O bending mode is shifted to higher frequencies (blue shift) for the confined water molecules irrespective of whether they are present within the cores or at the exterior surfaces of the Aβ aggregates. A blue shift in frequency by $\sim 15\,\mathrm{cm}^{-1}$ is observed for the water molecules present at the exterior surface of the protofilaments. It is found that the $\sim 50\,\mathrm{cm}^{-1}$ band for water molecules confined inside the cores of lower order aggregates (O_5 and O_8) is further blue shifted as compared to the surface water. This indicates increasingly restricted transverse oscillations of water confined within more rigid core environment of smaller protofilaments. In contrast, compared to the surface water, we do not see any noticeable shift for

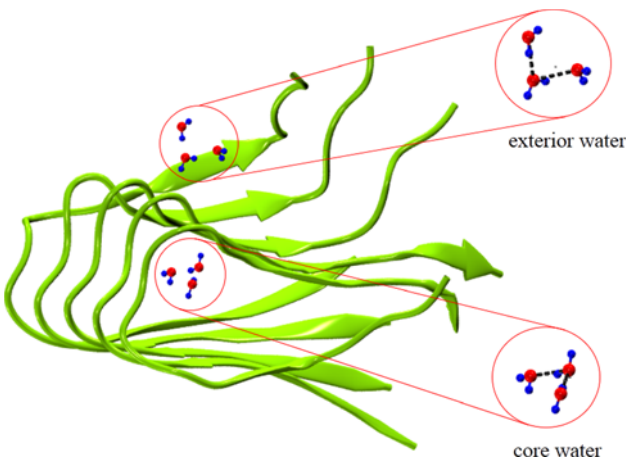

Figure 3. A representative snapshot of the core and exterior water molecules in pentameric unit (O_5) showing O···O···O bending mode of the oxygen atoms.

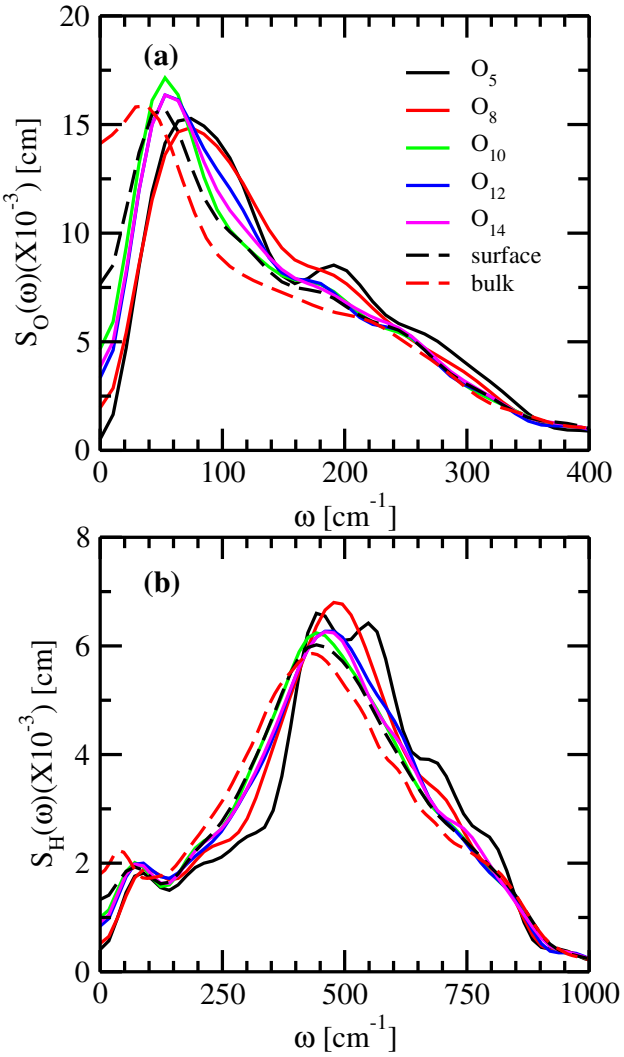

Figure 4. (a) Power spectra, $S_O(\omega)$, obtained by the Fourier transformation of the velocity autocorrelation function, $C_V^O(t)$, for the oxygen atoms of the water molecules that are present within the cores of different Aβ protofilaments. (b) The corresponding power spectra, $S_H(\omega)$, for the hydrogen atoms of those water molecules. The respective results for the surface water molecules as obtained by averaging over the protofilaments and that for water in pure bulk state are shown in each of the panels for comparison.

the corresponding band for higher order Aβ protofilaments (O_{10} onward). However, the intensities of the bands are significantly enhanced for the core water. Interestingly, formation of the protofilament does not seem to have much influence on the water intermolecular stretching at $\sim 200\,cm^{-1}$. However, the intensity of the band increases for water confined in and around the protofilaments, the effect being more for the core water. Such amplified intensity of the $200\,cm^{-1}$ band originates from increasingly restricted longitudinal motions of the core water due to confinement, the effect is particularly noticeable for the lower order aggregates (O_5 and O_8). Note that the intensity of $S_O(\omega)$ at zero frequency ($\omega = 0$) provides a measure of diffusion coefficient. Significantly lower intensities at zero frequency for water molecules present either at the exterior surfaces or confined within the cores of the Aβ aggregates correlate well with the restricted translational mobilities of those as reported earlier.[30] Further, it can be seen that such zero frequency intensity for the core water spectra increases with increase in size of the aggregates, except for O_{10}. This is an important observation which signifies that O_{10} being the crossover point exhibits anomalous behavior. Here, it may be noted that the calculation of diffusion coefficients from the zero frequency intensity of VDOS may often be ambiguous as long tail relaxations are not generally considered for the construction of VDOS.[44] However, the relative intensities at zero frequency as obtained from our present results are consistent with that found in our previous work, especially the anomalous nature of the core waters of O_{10}.[30]

The band corresponding to $500\,cm^{-1}$ in Figure 4(b) provides interesting result. Water molecules present at the exterior surfaces of the protofilaments do not exhibit any shift of the hydrogen bond power spectra ($S_H(\omega)$) as compared to pure bulk water. However, restricted librational motions are evident from increased intensities of the band. On the other hand, in addition to increased intensity, the band is also found to be blue shifted by $\sim 50\,cm^{-1}$ for the core water. Besides, intensities of the band are observed to be sensitive to the available core volume. Interestingly, no shift in the $500\,cm^{-1}$ band for the core water in crossover protofilament O_{10} is noticed. Moreover, the spectra of the hydrogen atoms of the core water in O_{10} are found to be quite similar to that of the surface water except at the peak position where the O_{10} core water exhibits relatively higher intensity. Such almost identical spectral pattern between the core and the surface water molecules around O_{10} indicates that the exchange between the core and the surface water molecules is easily feasible due to reduction in restriction in the confinement in its core region. Thus, it once again re-iterates the fact that O_{10} serves as crossover point where structural transformation begins to take place in order to transform into more stable structure, which is consistent with our earlier works.[29,30,41]

Next, we explore the low-frequency vibrational density of states ($S_O(\omega)$ and $S_H(\omega)$) of the water molecules that are bound to the Aβ peptide residues by PW hydrogen bonds. The results for water molecules confined within the cores of five Aβ protofilaments are depicted in Figure 5. Again, the

corresponding data for surface water averaged over all the protofilaments and that for water in pure bulk state are included in the figure for comparison. The results show that except for O_5 core water, the peak positions of the O · · · O · · · O bending mode are shifted further toward higher frequency by $\sim 10\,cm^{-1}$ as compared to that observed in Figure 4(a). This once again confirms stronger caging effects of the bound water molecules. Note that the results for O_5 core water are not affected, as most of those water molecules are bound to the peptide residues by hydrogen bonds. It is

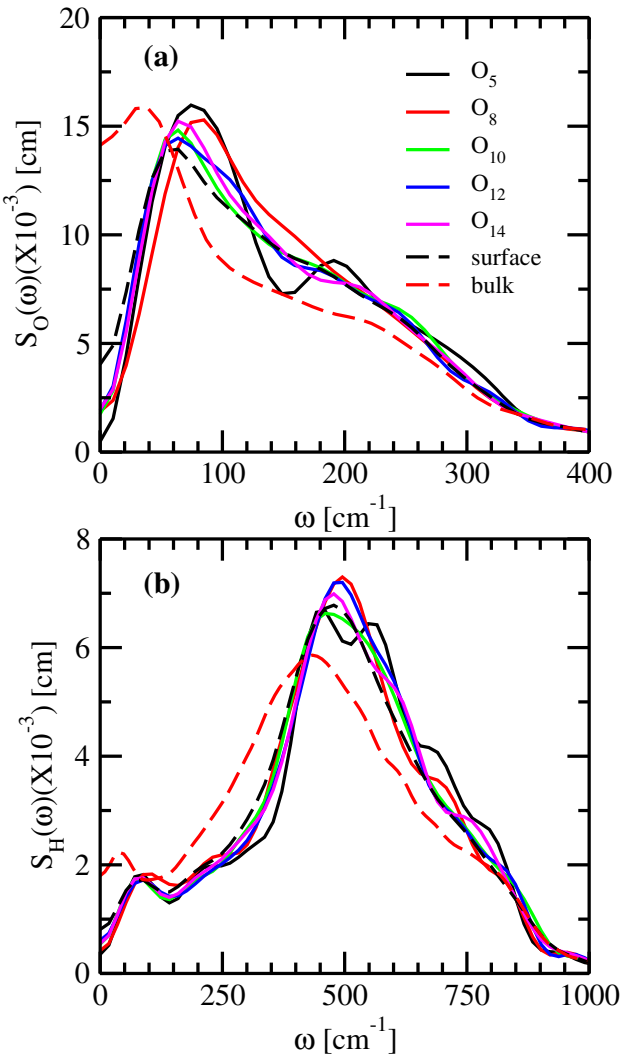

Figure 5. (a) Power spectra, $S_O(\omega)$, obtained by the Fourier transformation of the velocity autocorrelation function, $C_V^O(t)$, for the oxygen atoms of the water molecules that are hydrogen bonded with the peptide atoms and present within the cores of different Aβ protofilaments. (b) The corresponding power spectra, $S_H(\omega)$, for the hydrogen atoms of such bound water molecules. The respective results for the surface water molecules as obtained by averaging over the protofilaments and that for water in pure bulk state are shown in each of the panels for comparison.

further noticed that though the O · · · O stretching band positions for the bound waters around $200cm^{-1}$ are not influenced as such, but, compared to Figure 4(a), noticeable increase in the intensities of the band can be seen. Once again, the relative intensities of the spectra as obtained in the present study correlates well with the time scale of hydrogen bond dynamics as reported in our earlier work.[30] This suggests increasingly restricted longitudinal oscillations of the water molecules that are bound with the Aβ aggregates by hydrogen bonds. The influence on the librational motions of the bound water molecules is found to be interesting. We notice from Figure 5(b) that the band corresponding to $500\,cm^{-1}$ shifts to higher frequency by $\sim 40\,cm^{-1}$ for those water molecules that are present at the exterior surface of the Aβ protofilaments and bound by PW hydrogen bonds. Besides, the enhancement of the intensity of the band indicates restricted librational motions of the surface water on formation of PW hydrogen bonds. Surprisingly, on the other hand, no noticeable shift for the core waters involved in PW hydrogen bonds as compared to Figure 4(b) where all the waters were considered. This shows that most of the water molecules confined within the cores are either hydrogen bonded to the peptides or remain within the hydrogen bonding distance.

4. Conclusions

In this work, we have carried out MD simulations of aggregated $A\beta_{17-42}$ protofilaments of different sizes ranging from pentamer (O_5) to tetradecamer (O_{14}) in aqueous solutions to probe the effect of confinement within their hydrated nanocores as well as at the exterior surfaces on the low-frequency vibrational spectra of water molecules. In particular, attempts have been made to quantify how the non-uniform structural distortions of the Aβ protofilaments influence the low-frequency vibrational modes of the confined water molecules.

The calculations revealed enhanced back scattering of water molecules irrespective of whether they are present at the exterior surfaces or confined within the nanocores of the Aβ protofilaments. The extent of such back scattering has been found to be significantly higher for the core water molecules. Besides, it is demonstrated that the effect of confinement on the VDOS of the core water molecules is highly heterogeneous, as opposed to near-identical behavior of the surface water molecules. The extent of water back scattering is found to be maximum within the nanocores

of the lower order protofilaments (O_5 and O_8) due to severely constrained topology inside their cores. Importantly, water back scattering within O_{10} core is minimum due to its large scale distortion with a consequent expanded core volume. Such minimum back scattering effect leads to maximum diffusivity of O_{10} core water among all the protofilaments, which is consistent with our earlier studies.[29,30,41] It is further demonstrated that the O · · · O · · · O bending mode of water present in and around the protofilaments is blue shifted due to enhanced back scattering. Such blue shifts are found to be higher for the core water molecules, the effect is greater for the more rigid lower order Aβ aggregates, O_5 and O_8. It is observed that the extent of blue shift increases further for the water molecules that are bound to the peptides by PW hydrogen bonds. Interestingly, in contrast to the O · · · O · · · O bending mode, presence of Aβ protofilaments does not have any detectable influence on the position of O · · · O stretching mode of water. Our results further demonstrated hindered librational motions of the water molecules present within the cores of the protofilaments due to the confined environment and their propensity to remain bound with the peptides by PW hydrogen bonds.

We believe that size-dependent shift in the band positions of the low-frequency vibrational spectra of core water molecules as observed in the present study can be an effective indicator in determining the protofilament size and hence monitoring the aggregation process of Aβ peptides. Therefore, THz spectroscopy measurements on such systems can be performed to validate our results and to accurately establish the aggregation mechanism.

Acknowledgements

This study was supported by grants from the Department of Science and Technology (DST), Government of India, under the DST-FIST programme (SR/FST/CSII-011/2005, SR/FST/CSII-026/2013). PK thanks University Grants Commission (UGC), Government of India (18-12/2011(ii)EU-V, dated 16/08/2012), while SM thanks the Council of Scientific and Industrial Research (CSIR) Government of India (09/081(1272)/2015-EMR-I, dated 29.12.2015) for providing scholarships.

References

1. Uversky V N, Oldfield C J and Dunker A K 2008 Intrinsically disordered proteins in human diseases: Introducing the d2 concept *Annu. Rev. Biophys.* **37** 215
2. Chiti F and Dobson C M 2006 Protein misfolding, functional amyloid, and human disease *Annu. Rev. Biochem.* **75** 333
3. Hartl FU, Bracher A and Hayer-Hartl M 2011 Molecular chaperones in protein folding and proteostasis *Nature* **475** 324
4. Nunan J and Small D H 2000 Regulation of app cleavage by α-, β-and γ-secretases *FEBS Lett.* **483** 6
5. Haass C and Selkoe D J 2007 Soluble protein oligomers in neurodegeneration: Lessons from the alzheimer's amyloid β-peptide *Nat. Rev. Mol. Cell Biol.* **8** 101
6. Riek R, Güntert P, Döbeli H, Wipf B and Wüthrich K 2001 Nmr studies in aqueous solution fail to identify significant conformational differences between the monomeric forms of two alzheimer peptides with widely different plaque-competence, aβ (1–40) ox and aβ (1–42) ox *Eur. J. Biochem.* **268** 5930
7. Hartmann T, Bieger S C, Brühl B, Tienari P J, Ida N, Allsop D, Roberts G W, Masters C L, Dotti C G, Unsicker K and Beyreuther K 1997 Distinct sites of intracellular production for alzheimer's disease aβ40/42 amyloid peptides *Nature Med.* **3** 1016
8. Kayed R, Head E, Thompson J L, McIntire T M, Milton S C, Cotman C W and Glabe C G 2003 Common structure of soluble amyloid oligomers implies common mechanism of pathogenesis *Science* **300** 486
9. Tiraboschi P, Hansen L, Thal L and Corey-Bloom J 2004 The importance of neuritic plaques and tangles to the development and evolution of ad *Neurology* **62** 1984
10. Kayed R, Sokolov Y, Edmonds B, McIntire T M, Milton S C, Hall J E and Glabe C G 2004 Permeabilization of lipid bilayers is a common conformation-dependent activity of soluble amyloid oligomers in protein misfolding diseases *J. Biol. Chem.* **279** 46363
11. Lesné S, Koh M T, Kotilinek L, Kayed R, Glabe C G, Yang A, Gallagher M and Ashe K H 2006 A specific amyloid-β protein assembly in the brain impairs memory *Nature* **440** 352
12. Wasling P, Daborg J, Riebe I, Andersson M, Portelius E, Blennow K, Hanse E and Zetterberg H 2009 Synaptic retrogenesis and amyloid-beta in Alzheimer's disease *J. Alzheimer's Dis.* **16** 1
13. Krone M G, Hua L, Soto P, Zhou R, Berne B and Shea J E 2008 Role of water in mediating the assembly of alzheimer amyloid-β aβ16-22 protofilaments *J. Am. Chem. Soc.* **130** 11066
14. Thirumalai D, Reddy G and Straub J E 2012 Role of water in protein aggregation and amyloid polymorphism *Acc. Chem. Res.* **45** 83
15. Chong S H and Ham S 2012 Impact of chemical heterogeneity on protein self-assembly in water *Proc. Natl. Acad. Sci. U. S. A.* **109** 7636
16. Khatua P, Jose J C, Sengupta N and Bandyopadhyay S 2016 Conformational features of the aβ_{42} peptide monomer and its interaction with the surrounding solvent *Phys. Chem. Chem. Phys.* **18** 30144
17. Buchete N V, Tycko R and Hummer G 2005 Molecular dynamics simulations of Alzheimer's β-amyloid protofilaments *J. Mol. Biol.* **353** 804
18. Zheng J, Jang H, Ma B, Tsai C J and Nussinov R 2007 Modeling the alzheimer aβ_{17-42} fibril architecture: Tight intermolecular sheet-sheet association and intramolecular hydrated cavities *Biophys. J.* **93** 3046
19. Paravastu A K, Qahwash I, Leapman R D, Meredith S C and Tycko R 2009 Seeded growth of β-amyloid fibrils

from alzheimer's brain-derived fibrils produces a distinct fibril structure *Proc. Natl. Acad. Sci. U. S. A.* **106** 7443
20. Kirschner D A, Abraham C and Selkoe D J 1986 X-ray diffraction from intraneuronal paired helical filaments and extraneuronal amyloid fibers in Alzheimer disease indicates cross-beta conformation *Proc. Natl. Acad. Sci. U. S. A.* **83** 503
21. Balbach J J, Petkova A T, Oyler N A, Antzutkin O N, Gordon D J, Meredith S C and Tycko R 2002 Supramolecular structure in full-length Alzheimer's β-amyloid fibrils: Evidence for a parallel β-sheet organization from solid-state nuclear magnetic resonance *Biophys. J.* **83** 1205
22. Petkova A T, Leapman R D, Guo Z, Yau W M, Mattson M P, Tycko R 2005 Self-propagating, molecular-level polymorphism in Alzheimer's ß-amyloid fibrils *Science* **307** 262
23. Lührs T, Ritter C, Adrian M, Riek-Loher D, Bohrmann B, Döbeli H, Schubert D and Riek R 2005 3d structure of Alzheimer's amyloid-β (1–42) fibrils *Proc. Natl. Acad. Sci. U. S. A.* **102** 17342
24. Tarus B, Straub J E and Thirumalai D 2006 Dynamics of asp23-lys28 salt-bridge formation in aβ_{10-35} monomers *J. Am. Chem. Soc.* **128** 16159
25. Sciarretta K L, Gordon D J, Petkova A T, Tycko R and Meredith S C 2005 A β40-lactam(d23/k28) models a conformation highly favorable for nucleation of amyloid *Biochemistry* **44** 6003
26. Reddy G, Straub J E and Thirumalai D 2009 Influence of preformed asp23–lys28 salt bridge on the conformational fluctuations of monomers and dimers of aβ peptides with implications for rates of fibril formation *J. Phys. Chem. B* **113** 1162
27. Kahler A, Sticht H and Horn A H 2013 Conformational stability of fibrillar amyloid-beta oligomers via protofilament pair formation-a systematic computational study *PLoS ONE***8** e70521
28. GhattyVenkataKrishna P K and Mostofian B 2013 Dynamics of water in the amphiphilic pore of amyloid β fibrils *Chem. Phys. Lett.* **582** 1
29. Khatua P and Bandyopadhyay S 2018a Understanding the microscopic origin behind heterogeneous properties of water confined in and around aβ_{17-42} protofilaments *J. Chem. Phys.* **149** 065101
30. Khatua P and Bandyopadhyay S 2018b Dynamical crossover of water confined within the amphiphilic nanocores of aggregated amyloid β peptides *Phys. Chem. Chem. Phys.* **20** 14835
31. Walrafen G and Chu Y 1995 Linearity between structural correlation length and correlated-proton Raman intensity from amorphous ice and supercooled water up to dense supercritical steam *J. Phys. Chem.* **99** 11225
32. Walrafen G, Chu Y and Piermarini G 1996 Low-frequency Raman scattering from water at high pressures and high temperatures *J. Phys. Chem.* **100** 10363
33. Martì J, Padro J and Guàrdia E 1996 Molecular dynamics simulation of liquid water along the coexistence curve: Hydrogen bonds and vibrational spectra *J. Chem. Phys.* **105** 639
34. Brubach J B, Mermet A, Filabozzi A, Gerschel A and Roy P 2005 Signatures of the hydrogen bonding in the infrared bands of water *J. Chem. Phys.* **122** 184509
35. Ebbinghaus S, Kim S J, Heyden M, Yu X, Heugen U, Gruebele M, Leitner D M and Havenith M 2007 An extended dynamical hydration shell around proteins *Proc. Natl. Acad. Sci. U. S. A.* **104** 20749
36. Meister K, Ebbinghaus S, Xu Y, Duman J G, DeVries A, Gruebele M, Leitner D M and Havenith M 2013 Long-range protein–water dynamics in hyperactive insect antifreeze proteins *Proc. Natl. Acad. Sci. U. S. A.* **110** 1617
37. Ebbinghaus S, Kim S J, Heyden M, Yu X, Gruebele M, Leitner D M and Havenith M 2008 Protein sequence- and ph-dependent hydration probed by terahertz spectroscopy *J. Am. Chem. Soc.* **130** 2374
38. Luong T Q, Xu Y, Bründermann E, Leitner D M and Havenith M 2016 Hydrophobic collapse induces changes in the collective protein and hydration low frequency modes *Chem. Phys. Lett.* **651** 1
39. Wirtz H, Schäfer S, Hoberg C, Reid K M, Leitner D M and Havenith M 2018 Hydrophobic collapse of ubiquitin generates rapid protein-water motions *Biochemistry***57** 3650
40. Phillips J C, Braun R, Wang W, Gumbart J, Tajkhorshid E, Villa E, Chipot C, Skeel R D, Kale L and Schulten K 2005 Scalable molecular dynamics with namd *J. Comput. Chem.* **26** 1781
41. Khatua P, Sinha S K and Bandyopadhyay S 2017 Size-dependent conformational features of aβ_{17-42} protofilaments from molecular simulation studies *J. Chem. Inf. Model.* **57** 2378
42. Feller S E, Zhang Y, Pastor R W and Brooks B R 1995 Constant pressure molecular dynamics simulation: The langevin piston method *J. Chem. Phys.* **103** 4613
43. Ryckaert J P, Ciccotti G and Berendsen H J 1977 Numerical integration of the cartesian equations of motion of a system with constraints: Molecular dynamics of n-alkanes *J. Comput. Phys.* **23** 327
44. Allen M P and Tildesley D J 1987 Computer Simulation of Liquids, Oxford University Press
45. Darden T, York D and Pedersen L 1993 Particle mesh ewald: An n log (n) method for ewald sums in large systems *J. Chem. Phys.* **98** 10089
46. MacKerell A D, Bashford D, Bellott M, Dunbrack R, Evanseck J, Field M J, Fischer S, Gao J, Guo H, Ha S, Joseph-McCarthy D, Kuchnir L, Kuczera K, Lau F T K, Mattos C, Michnick S, Ngo T, Nguyen D T, Prodhom B, Reiher W E, Roux B, Schlenkrich M, Smith J C, Stote R, Straub J, Watanabe M, Wiórkiewicz-Kuczera J, Yin D and Karplus M 1998 All-atom empirical potential for molecular modeling and dynamics studies of proteins *J. Phys. Chem. B* **102** 3586
47. MacKerell A D, Feig M and Brooks C L 2004 Extending the treatment of backbone energetics in protein force fields: Limitations of gas-phase quantum mechanics in reproducing protein conformational distributions in molecular dynamics simulations *J. Comput. Chem.* **25** 1400
48. Neria E, Fischer S and Karplus M 1996 Simulation of activation free energies in molecular systems *J. Chem. Phys.* **105** 1902
49. Jorgensen W L, Chandrasekhar J, Madura J D, Impey R W and Klein M L 1983 Comparison of simple potential

functions for simulating liquid water *J. Chem. Phys.* **79** 926
50. Jose J C, Khatua P, Bansal N, Sengupta N and Bandyopadhyay S 2014 Microscopic hydration properties of the aβ1–42 peptide monomer and the globular protein ubiquitin: A comparative molecular dynamics study *J. Phys. Chem. B* **118** 11591
51. Gupta M, Khatua P, Chakravarty C and Bandyopadhyay S 2018 Hydration behavior along the folding pathways of Trpzip4, Trpzip5 and Trpzip6 *J. Phys. Chem. B* **122** 1560
52. Li J 1996 Inelastic neutron scattering studies of hydrogen bonding in ices *J. Chem. Phys.* **105** 6733
53. Crupi V, Dianoux A J, Majolino D, Migliardo P and Venuti V 2002 Dynamical response of liquid water in confined geometry by laser and neutron spectroscopies *Phys. Chem. Chem. Phys.* **4** 2768
54. Padró J À and Martì J 2003 An interpretation of the low-frequency spectrum of liquid water *J. Chem. Phys.* **118** 452
55. Svishchev I M and Kusalik P G 1994 Rotational dynamics in liquid water: A simulation study of librational motions *J. Chem. Soc. Faraday Trans.* **90** 1405